The Astrophysical Journal, 431:L75–L78, 1994 August 20

ABSORPTION IN 3C 212

Smita Mathur
Harvard-Smithsonian Center for Astrophysics, 60 Garden Street, Cambridge MA 02138
I: smita@cfa.harvard.edu
Received 1994 April 4; accepted 1994 June 1

ABSTRACT

3C 212 (Q0855+143) is a red quasar with ambiguous evidence for strong low-energy X-ray absorption in its *ROSAT* spectrum (Elvis et al. 1994). We combine *Einstein* and *ROSAT* data with ultraviolet absorption-line strengths to investigate the physical state of the absorber. We find that a highly ionized absorber ($U \sim 0.3$) provides a consistent fit to both X-ray and UV data as well as providing a significantly improved fit to the X-ray spectrum. The absorber is outflowing with a velocity of ~ 1600 km s^{-1} with respect to the Mg II emission line, situated outside the broad emission-line region (BELR) and has low density. The alternative blackbody fit to the X-ray data is excluded if the source has not varied, and it is also unable to predict the UV absorption lines. This is the second case of an X-ray absorber identified with a UV absorber (the first one being 3C 351; Mathur et al. 1994) and suggests that UV/X-ray absorbers may be common. This is an exciting possibility as the combination of UV and X-ray constraints is very powerful in determining the physical conditions of an absorber.

Subject headings: quasars: absorption lines — quasars: individual (3C 212) — X-rays: galaxies

1. INTRODUCTION

The puzzle of the nature of the red quasars (e.g., Smith & Spinrad 1980) was partly resolved by the discovery that the *ROSAT* X-ray spectrum of the $z = 1.049$ red quasar 3C 212 has a strong low-energy cutoff (Elvis et al. 1994, hereafter Paper I). The spectrum can be fitted with a power law (of energy index $1.4^{+0.8}_{-0.6}$) with low-energy photoelectric absorption in excess of the Galactic value which, if at the redshift of the quasar, would have a column density of $(0.87^{+0.8}_{-0.6}) \times 10^{22}$ atoms cm^{-2}. The implied absorbing column density may include sufficient dust to redden a normal quasar spectrum to the observed steep optical slope of 3C 212. However, an alternative acceptable fit to the X-ray spectrum is a blackbody with a temperature of 0.7 keV (in the quasar frame) modified only by Galactic absorption. Although a blackbody spectrum would be unprecedented, the model is consistent with the *ROSAT* X-ray and optical data and could not be ruled out (Paper I).

Two additional pieces of data are available:

1. 3C 212 was also observed by the *Einstein* IPC. The higher energy range of the IPC (0.2–4 keV) as compared to the PSPC (0.1–2 keV) could, in principle, allow discrimination between the two models. We have reanalyzed the *Einstein* IPC spectrum with this aim in mind.

2. Associated Mg II absorption has been observed in the optical (rest frame UV) spectrum of 3C 212 (Aldcroft, Bechtold, & Elvis 1994a). Mathur et al. (1994) have demonstrated the great advantage in determining the properties of the absorber that is afforded by the combination of UV and X-ray data. In the case of 3C 351, they demonstrated that the absorption as seen in X-rays is due to the same material responsible for UV model-line absorption.

In this *Letter* we investigate whether the same is true for 3C 212. We show that this is so and that the required ionized absorber improves the fit to the X-ray data.

2. THE X-RAY SPECTRUM FROM *Einstein* AND *ROSAT*

3C 212 was observed by the *Einstein* IPC on 1980 October 10 for 10,251 s (Bregman et al. 1985). The observed count rate was 0.038 counts s^{-1} for a total of 390 counts. The data were extracted from the *Einstein* Unscreened Data Archive. The standard data processing for the IPC rejected all of the exposure time for this observation because no star tracker aspect solution was obtained. In practice this is rarely a problem for IPC observations since the $\sim 75''$ FWHM of the IPC (Harris et al. 1990) is not blurred by the typical aspect errors of a few arcseconds incurred by observations that have an aspect solution based only on the gyro data. (Indeed, the gyro data alone were used to produce the *Einstein* Slew Survey [Elvis et al. 1992] which has typical positional errors of $\sim 1'$.) The image of 3C 212 has a FWHM consistent with a point source ($76''$) with no aspect smearing, verifying that there is no problem with aspect in this observation.

The source counts were extracted using IRAF PROS software package within a $3'$ radius circle centered on the X-ray source position. This size of circle allows proper correction for mirror scattering (Harnden et al. 1984). The source counts for 3C 212 did not increase for larger radii. Background counts were estimated within an annulus of $2'$ width at $4'$ radius centered on the source. Net source counts after background subtraction were 384 ± 41.5, sufficient to fit a simple spectrum. Model fits to the extracted counts were carried out using the well-calibrated channels 2–10 (0.2–4.4 keV). The χ^2 statistic was used to estimate the goodness of fit. Once again, power-law and blackbody models were both good fits to the data (Table 1). Thus, the *Einstein* data alone were unable to discriminate between the models.

Model fits to the combined PSPC and IPC data were then carried out using the XSPEC software package (details of the *ROSAT* observations and extraction of the source pulse height spectrum are given in Paper I). Channels 2–10 of IPC data and 3–34 of PSPC data were used. Channels with few counts

TABLE 1

SPECTRAL FITS TO THE PSPC AND IPC SPECTRA OF 3C 212[a]

Model Fitted	α_E or kT[b]	N_H(free)[c]	Normalization[d]	Other Parameter[e]	χ_r^2(dof)
IPC Only					
Power-Law:					
$+N_H(z=0, \text{free})$	$1.4^{+3.4}_{-1.1}$	$1.8^{+1.0}_{-0.0}$	$5.4^{+2.0}_{-2.9}$		0.98(6)
$+N_H(\text{Gal, fixed})$	$0.6^{+0.4}_{-0.4}$	...	$3.2^{+0.6}_{-0.7}$		1.0(7)
$+N_H(\text{Gal, fixed}) + N_H(z=1.049, \text{free})$	$1.3^{+3.3}_{-1.0}$	$7.3^{+56.4}_{-0.1}$	$5.3^{+0.7}_{-2.6}$		0.98(6)
Blackbody:					
$(z=1.049) + N_H(z=0, \text{free})$	$0.9^{+0.25}_{-0.35}$	$0.01^{+0.01}_{-0.01}$	$0.5^{+0.2}_{-0.2}$		1.13(6)
$(z=1.049) + N_H(\text{Gal, fixed})$	$0.8^{+0.3}_{-0.2}$	...	$0.5^{+0.9}_{-0.7}$		0.99(7)
PSPC + IPC					
Power-Law:					
$+N_H(z=0, \text{free})$	$1.7^{+1.0}_{-0.7}$	$2.7^{+2.0}_{-1.3}$	$3.7^{+2.7}_{-1.2}$	$7.1^{+6.5}_{-2.7}$	0.71(29)
$+N_H(\text{Gal, fixed})$	$0.2^{+0.1}_{-0.1}$	...	$1.8^{+0.1}_{-0.1}$	$2.6^{+0.4}_{-0.4}$	1.4(30)
$+N_H(\text{Gal, fixed}) + N_H(z=1.049, \text{free})$	$1.4^{+0.7}_{-0.7}$	$8.7^{+7.4}_{-6.1}$	$3.0^{+1.3}_{-0.9}$	$5.6^{+3.3}_{-2.1}$	0.73(29)
Same as above[f]	$0.6^{+0.6}_{-0.3}$	$2.5^{+0.5}_{-0.2}$	$2.2^{+0.7}_{-0.3}$	$2.2^{+0.7}_{-0.3}$	1.46(30)
Blackbody:					
$(z=1.049) + N_H(z=0, \text{free})$	$0.7^{+0.1}_{-0.1}$	$0.2^{+0.5}_{-0.2}$	$2.6^{+0.3}_{-0.2}$	$5.4^{+0.9}_{-0.8}$	0.73(29)
$(z=1.049) + N_H(\text{Gal, fixed})$	$0.7^{+0.1}_{-0.1}$	...	$2.7^{+0.2}_{-0.2}$	$5.5^{+0.8}_{-0.8}$	0.73(30)
Same as above[f]	$0.7^{+0.1}_{-0.1}$	...	$0.3^{+0.03}_{-0.02}$	$0.3^{+0.03}_{-0.02}$	1.8(31)
PSPC Only					
Power-Law:					
$+N_H(\text{Gal, fixed}) + N_H(z=1.049, \text{free})$	$1.4^{+0.8}_{-0.6}$	$8.7^{+7.5}_{-6.3}$	$3.0^{+1.4}_{-0.9}$		0.72(21)
$+\text{Edge}(z=1.049, 0.74\ \text{keV})$	$1.5^{+0.7}_{-0.6}$	$3.6^{+2.7}_{-1.6}$	$3.0^{+1.1}_{-0.7}$	$3.9^{+3.9}_{-3.0}$	0.59(20)

[a] χ_r^2 is per dof. Errors are 68% for two interesting parameters.
[b] α_E is the energy spectral index (f = Norm. $E^{-\alpha E}$); temperatures are in keV.
[c] N_H is in 10^{21} atoms cm^{-2}.
[d] Normalization units are for power-law fits: 10^{-4} keV cm^{-2} s^{-1} keV^{-1} at 1 keV; and for blackbody fits: 10^{-4} keV cm^{-2} s^{-1} at kT keV.
[e] Other parameter is IPC normalization in the case of PSPC + IPC spectrum, and it is the optical depth for the model with an edge.
[f] Relative PSPC and IPC normalization is fixed to be 1.

were combined to ensure at least 10 counts per channel (see Paper I). We attempted to fit the same spectral shape to both the data sets leaving the relative normalization free. Power-law and blackbody models were again both good fits to the combined data set (Table 1) with IPC normalization larger by about a factor of 2 than the PSPC. Excess absorption is clearly indicated in the power-law models. A power-law fit with a $z = 0$ absorption component fixed at Galactic value plus another absorption component, which was allowed to vary at the redshift of 3C 212, provides a very good fit (Table 1), as in Paper I. If the combined data set is fitted with the same spectral shape and normalization, the fits become worse (Table 1). For the power-law fit, the reduced χ_r^2 (1.46) is barely acceptable ($P = 5\%$), while for the blackbody fit $\chi_r^2 = 1.8$ is clearly unacceptable ($P \sim 0.5\%$). This may partly be due to the systematic uncertainty in the relative calibrations of the PSPC and IPC (Fiore et al. 1994) or to variability in the decade between the observations.

The analysis of IPC data in combination with PSPC remains inconclusive in discriminating between the models, although fits with a power-law model were generally preferred. Intrinsic absorption at the source was required by the power-law model. As discussed in Paper I, this large column of gas in the quasar may account for the large reddening observed in 3C 212. In the following section we explore the possibility of the same gas also being responsible for the associated Mg II absorption in the source.

3. ASSOCIATED Mg II ABSORPTION

Aldcroft et al. (1994a) have discovered an associated Mg II absorption system in 3C 212 at $z_{abs} = 1.049$ which corresponds to an outflow velocity of 1600 km s^{-1} with respect to the Mg II emission-line redshift of the quasar. The rest frame equivalent widths for the Mg II doublet in absorption are 0.76 and 0.50 Å for Mg II λ2796 and Mg II λ2803, respectively. We followed the techniques developed in Mathur et al. (1994) to solve for physical conditions consistent with both the Mg II and X-ray absorption. The width of the absorption lines was limited by the spectral resolution ($\lesssim$6 Å). The absorbing column density of Mg II was calculated using standard curve-of-growth techniques (e.g., Spitzer 1978). The observed doublet ratio $W(2796)/W(2803) = 1.5$ compared to the natural ratio of 2.0. Minimum Mg II column density is thus derived by assuming that the absorption lines lie on the linear part of the curve-of-growth; $M(\text{Mg II}) > 2.3 \times 10^{13}$ cm^{-2}. Assuming a solar abundance of magnesium relative to hydrogen (3.8×10^{-5}; Grevesse & Anders 1989), the equivalent column density of hydrogen is $N_H = 6.1 \times 10^{17}/f_{\text{Mg II}}$ cm^{-2}, where $f_{\text{Mg II}}$ is the fraction of magnesium in Mg II state of ionization. If the Mg II absorber is the same as the X-ray absorber, the strong constraint on total N_H provided by the X-ray data ($N_H = 8.7^{+0.8}_{-0.6} \times 10^{21}$ cm^{-2}; Table 1) determines the ionization fraction of magnesium to be very low ($\log f_{\text{Mg II}} = -4.15$). The exact values of Mg II column density and $f_{\text{Mg II}}$ depend strongly on

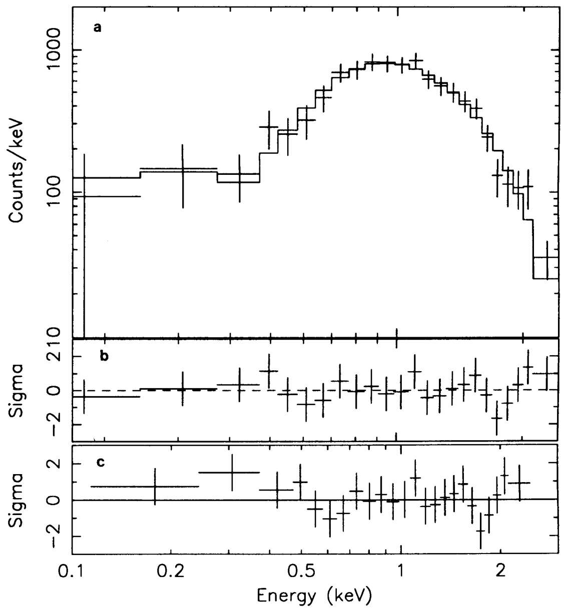

FIG. 1.—*ROSAT* PSPC spectrum of 3C 212 (*a*) with the model of a power law with Galactic (fixed) and $z = 1.049$ absorption with an edge at 0.74 keV (rest frame), (*b*) residuals after subtraction of the model, and (*c*) residuals after subtraction of the model without an edge (Paper I).

the velocity spread parameter "*b*" in the curve-of-growth analysis, and $N_{\rm Mg\,II}$ can be larger by orders of magnitude if it lies on the flat portion of the curve of growth. However, the main results of this *Letter* would still be valid, as shown below. High-resolution observations are needed to fit "*b*" and $N_{\rm ion}$ independently.

In the context of photoionization models, we look for a consistent solution for an absorbing gas cloud satisfying the above constraints. Photoionization models predict $f_{\rm ion}$ given the input continuum, column density, number density ($n_{\rm H}$), and the ionization parameter (U) of the gas ($U = Q/4\pi R^2 n_{\rm H} c$, where Q is the total number of ionizing photons per second). We constructed a grid of photoionization models for a range of ionization parameters using CLOUDY (Ferland 1991). The column density was fixed at the best-fit X-ray value. Mathur (1994) and Mathur et al. (1994) have demonstrated the importance of using the observed quasar continuum as opposed to a "standard" continuum. A 3C 212 continuum dereddened by $A_V = 2.8$, appropriate to the X-ray column assuming Galactic gas-to-dust ratio (see Paper I, Fig. 4) was used as the input continuum. Values of $f_{\rm ion}$ are insensitive to the choice of density for a given ionization parameter. Hence, the density was varied only between 10^9 and 10^5 cm^{-3}.

In principle, a low value of $f_{\rm Mg\,II}$ is possible either for a very low value of U when magnesium is mostly neutral with a small fraction in the Mg II state; or for a very large value of U when magnesium is highly ionized with a small fraction in the Mg II state and essentially no neutral magnesium. However, in order to remain neutral the material must be at least $\sim$100 kpc from the quasar continuum source. This is not impossible, but the neutral option can be ruled out observationally. Mg I λ2852 was within the wavelength range of observation by Aldcroft et al. (1994a), but the absorption line was not detected (EW < 0.1 Å). VLA 21 cm observations towards 3C 212 found no excess absorption above the detection limit of 10^{19} cm^{-2} (Aldcroft, Elvis, & Bechtold 1994b). Thus a mostly neutral absorber with a column density of 8.7×10^{21} cm^{-2}, either associated or intervening, can be ruled out.

On the other hand, a high value of U ($U \sim 0.3$), where Mg VIII is the dominant stage of ionization, provides a good fit. For this U, $n_{\rm H} R^2 = 10^5$ cm^{-3} kpc^2, where R is the distance from the central continuum. Dust can survive in such a cloud if $n_{\rm H} \lesssim 10^9$ cm^{-3} (Laor & Draine 1993, eq. [60]) constraining the distance of the absorber $R \gtrsim 10$ pc. If $N_{\rm Mg\,II}$ is larger by an order of magnitude (depending upon the "*b*" value), the resulting U would be $\sim$0.2 and $R \gtrsim 12$ pc.

3.1. *Model Predictions*

The X-ray/UV absorber is highly ionized with essentially no neutral magnesium, and thus Mg I absorption is not expected to occur. In this system, hydrogen is highly ionized with log $f_{\rm H\,I} = -4.94$. The column density of neutral hydrogen is thus only $\sim 10^{17}$ cm^{-3}, implying no 21 cm absorption toward 3C 212. C IV and O VI have large enough column density for absorption to be detected (predicted EW $\gtrsim 0.6$ Å) but lie outside the observed wavelength range. *HST* observations would be required to observe these lines.

Since the absorber in 3C 212 is partially ionized with $U \sim 0.3$, the low-energy X-ray absorption is not due to cold gas as assumed in the earlier X-ray spectral fitting. Instead, it is caused by the residual He and metal opacity of a "warm absorber" (Halpern 1984; Fiore et al. 1994; Mathur et al. 1994). The fractional abundance of He and He$^+$ is $\sim 4 \times 10^{-6}$ and 0.2, respectively. The relative abundances of O VII and O VIII predicted by the model are 0.36 and 0.01, respectively, O VII being the dominant stage of ionization of oxygen. Thus the transmitted spectrum should have absorption edges due to O VII/O VIII at 0.74/0.87 keV (rest frame). We thus refitted the PSPC spectrum with a model containing a power-law, Galactic absorption, intrinsic absorption, as before, adding an absorption edge at 0.74 keV at the source (Table 1). The fit was excellent with $\chi^2 = 11.82$ for 20 degrees of freedom (Fig. 1). This is a significant improvement over the earlier fit with a powr law and intrinsic absorption (Paper I) at 98% confidence using an F-test (Bevington & Robinson 1992). Thus, a warm absorber in 3C 212 is consistent with our identification of the Mg II absorber with the soft X-ray absorber. We conclude that all the observations are consistent with the X-ray absorption and the Mg II absorption occurring in the same gas.

Both X-ray and UV constraints can then be combined to derive the physical characteristics of the absorber. As described above, the absorber is outflowing with a velocity of $\sim$1600 km s^{-1}, has $U \lesssim 0.3$, $N_{\rm H} = 8.7^{+0.8}_{-0.6} \times 10^{21}$ cm^{-2} and $R \gtrsim 10$ pc. That places the absorber outside the broad emission-line region (BELR) which has $R \sim \frac{1}{3}$ pc. Depth of such an absorber would then be $\Delta R \gtrsim 9 \times 10^{12}$ cm, and the mass of a shell at R, about 8×10^5 $M_\odot$. For a covering factor of 1%, the mass loss rate is 1.2 $M_\odot$ yr^{-1} which is comparable to the accretion rate of 2 $M_\odot$ yr^{-1}. The kinetic luminosity of the outflow is $\sim 10^{44}$ ergs s^{-1}, only about 10^{-2} to 10^{-3} of the radiative luminosity.

4. CONCLUSIONS

We have shown that X-ray spectrum of 3C 212 is most likely a power law with intrinsic, partially ionized absorption ($N_{\rm H} = 8.7^{+0.8}_{-0.6} \times 10^{21}$ cm^{-2}, $U = 0.3$). Low-energy X-ray absorption in the spectra of active galactic nuclei was generally thought to be due to "cold" material due to the lack of any other information on the ionization state of the absorber. In our model, the absorber is required to be partially ionized ($U \sim 0.3$) and is responsible for both the low-energy X-ray absorption and the Mg II absorption. The absorber is associated with the quasar itself. It is situated outside the BELR and is outflowing with a velocity of ~ 1600 km s^{-1}. Thus the identification of Mg II absorber with the X-ray absorber in 3C 212 changes our understanding of the low-energy absorption in the X-ray spectrum of this peculiar "red" quasar.

This second success in a joint analysis of the UV and X-ray absorbers exemplifies the power in the technique. Even when the X-ray data itself are inadequate, many more cases of ionized absorbers will be identified in this way, and the large number of derivable physical parameters will allow us to understand the origin of this material and its role in active galactic nuclei.

It is my great pleasure to thank B. Wilkes and M. Elvis for their support and encouragement. I thank A. Prestwich, J. McDowell, D. Plummer, M. Garcia, and the staff of the *Einstein* Data Center for making the unscreened data available; A. Siemiginowska and S. Daines for installing and helping with the new XPEC package; and Tom Aldcroft for useful discussions. I an grateful to G. Ferland for providing us with his photoionization code CLOUDY. This work was supported by grant NAGW-2201 (LTSA).

REFERENCES

Aldcroft, T., Bechtold, J., & Elvis, M. 1994a, ApJS, 93, 1
Aldroft, T., Elvis, M., & Bechtold, J. 1994b, in preparation
Bevington, P., & Robinson, D. K. 1992, Data Reduction and Error Analysis for the Physical Sciences (New York: McGraw-Hill)
Bregman, J. N., Glassgold, A. E., Huggins, P. J., & Kinney, A. L. 1985, ApJ, 291, 505
Elvis, M., Fiore, F., Mathur, S., & Wilkes, B. 1994, ApJ, 425, 103 (Paper I)
Elvis, M., Plummer, D., Schachter, J., & Fabbiano, G. 1992, ApJS, 80, 257
Ferland, G. F. 1991, "HAZY" (OSU Astronomy Department Internal Report)
Fiore, F., Elvis, M., McDowell, J., Siemiginowska, A., & Wilkes, B. 1994, ApJ, 431, 515
Grevesse, N., & Anders, E. 1989, in Cosmic Abundances of Matter, ed. C. J. Waddington (New York: AIP), 1
Halpern, J. P. 1984, ApJ, 281, 90
Harnden, F. R., Fabricant, D. G., Harris, D. E., & Schwarz, J. 1984, SAO Report, 393
Harris, D., et al. 1990, The *Einstein* Catalog Committee, The *Einstein Observatory* Catalog of IPC X-Ray Sources 1990 (NASA Publication TM 108401), 102
Laor, A., & Draine, B. T. 1993, ApJ, 402, 441
Mathur, S. 1994, in IAU Symp. 159, Multiwavelength Continuum Emission of AGN, ed. T.-J. L. Courvoisier & A. Blecha (Dordrecht: Kluwer), 271
Mathur, S., Wilkes, B., Elvis, M., & Fiore, F. 1994, ApJ, in press
Smith, H. E., & Spinrad, H. 1980, ApJ, 236, 419
Spitzer, L. 1978, Physical Processes in the Interstellar Medium (New York: Wiley-Interscience)